Thermal and non-thermal photoinduced phenomena in α'-NaV_2O_5

2007 J. Phys.: Condens. Matter 19 076207

(http://iopscience.iop.org/0953-8984/19/7/076207)

IOP PUBLISHING JOURNAL OF PHYSICS: CONDENSED MATTER

J. Phys.: Condens. Matter **19** (2007) 076207 (11pp) doi:10.1088/0953-8984/19/7/076207

Thermal and non-thermal photoinduced phenomena in α'-NaV_2O_5

Tohru Suemoto, Hirokazu Nagase, Makoto Nakajima, Masahiko Isobe and Yutaka Ueda

Institute for Solid State Physics, The University of Tokyo, Kashiwanoha 5-1-5, Kashiwa-shi, Chiba, 277-8581, Japan

E-mail: suemoto@issp.u-tokyo.ac.jp

Received 4 August 2006, in final form 21 November 2006
Published 2 February 2007
Online at stacks.iop.org/JPhysCM/19/076207

Abstract

Transient reflectance changes induced by pulsed photo-excitation with 1.55 and 3.1 eV photons were studied in sodium vanadate, α'-NaV_2O_5. At low excitation densities, the response shows a slow rising with a time constant of 3 ps, while at higher excitation density, the rising becomes fast with a time constant of 500 fs. Oscillation in reflectance was also observed and ascribed to an acoustic phonon burst. The transient spectra were compared to the temperature difference reflectance spectra, and the photocreated states are understood as the high-temperature state of the high-temperature phase. On the other hand, the fast-rising components are ascribed to non-thermal creation of the charge-disordered phase.

1. Introduction

Recently, macroscopic changes of the material order induced by photo-excitation are receiving increasing attention. Laser annealing involves a transition from the solid state to the liquid state, and thermal and non-thermal liquidation has been found in several semiconductors [1]. As regards the photo-induced solid to solid phase transition, a neutral to ionic transition in TTF-chloranil [2–4], insulator to metal transition in $Pr_{0.7}Ca_{0.3}MnO_3$ [5], Mott transition in halogen-bridged Ni-complex [6], and charge-order disorder transition in $La_{0.5}Sr_{1.5}MnO_4$ [7] have been reported in the last decade. These phenomena are known as photo-induced phase transitions (PIPTs) [8].

In these cases, the role of heating due to laser irradiation is important, but it is sometimes very difficult to discriminate between thermal and non-thermal effects in the photo-induced phenomena. We have to consider two kinds of heating effects in repetitive pulsed light irradiation. One is the quasi-stationary increase of the sample temperature determined by the balance between the heat input at the irradiated volume of the sample and the cooling from the backside of the sample. The key parameter in this case is the heat conductivity. The other is the

transient heating, which is determined solely by heat capacity and the deposited heat energy in the excited volume.

In many of the time-resolved experiments of PIPTs, the excitation density ranges from 1×10^{18} to 3×10^{21} photons cm^{-3} or 0.3 to 700 J cm^{-3}, mostly of the order of 100 J cm^{-3} [3–5]. As the heat capacity of usual solid materials at room temperature falls around 2 J K^{-1} cm^{-3}, the energy deposited by the pump pulse will cause significant heating, if the energy is fully converted into heat energy. The effect will be even more serious at lower temperature, because the heat capacity decreases following the Debye's T-cubed law. Therefore, it is very important to pay equal attention to thermal and non-thermal effects in studying the photoinduced phenomena. In this paper, we study α'-NaV_2O_5, which is known to show a spin–Peierls-like phase transition accompanying a charge ordering at $T_c = 34$ K [9].

The crystal structure of α'-NaV_2O_5 consists of V_2O_5 sheets constructed by corner-sharing distorted VO_5 pyramids and sodium ions intercalated between these sheets. The vanadium ions in the sheet form a ladder structures with the legs running along the b-axis and the rungs lying along the a-axis. The V ions on the rung are bridged by an O ion. Neighbouring ladders are linked via common edges of the pyramids. Above 34 K, all the V ions have average charge of +4.5, while below this temperature, charge separation occurs, and the V^{4+} and V^{5+} ions make a double zigzag configuration on the ladder structure [10]. Simultaneously, the magnetic susceptibility decreases and a $2a \times 2b \times 4c$ superstructure appears in the x-ray diffraction pattern [11]. Optical properties such as reflectance spectra [12], Raman spectra [13] and infrared spectra [14] also change upon this phase transition. The phase transition has a second-order-type character; that is, the heat capacity shows a lambda-type peak at T_c and all the physical properties show a gradual change starting from several degrees below T_c.

The photoinduced phenomena in this material have been studied in our previous papers [15, 16] under relatively weak excitation density by pulses from a mode-locked Ti–sapphire laser. We discriminated between the quasi-stationary heating effect and the transient effect in pump and probe reflectance measurements. We suggested that a transient response with a rising time of about 3 ps might correspond to the phase transition from the low-temperature phase to a phase similar to the high-temperature phase. However, time-resolved Raman measurements directed us to a different interpretation [17]. The time evolution of the temperature within the laser spot was determined from Stokes to anti-Stokes Raman intensity ratio of the 66 cm^{-1} peak. It was shown that the transient temperature increase was 4 K and that it took about 5 ps to reach the equilibrium value [17], while the base temperature (quasi-stationary heating effect) was 19 K at an excitation fluence of 2 μJ cm^{-2} (repetition rate at 80 MHz). It was concluded that the reflectance change with a time constant of 3–5 ps corresponds to the temperature dependence of the reflectance within the low-temperature phase. The purpose of this paper is to clarify the dynamics of the thermal and non-thermal effects following photo-excitation in α'-NaV_2O_5.

2. Experiment

The samples we used were thin platelet single crystals, with a typical dimension of 1×2 mm^2 in the a–b plane, grown from melt, using the self-flux method. The sample was mounted on the cold finger of a He gas flow type cryostat (Oxford MicrostatHe). Amplified Ti sapphire laser pulses at 800 nm with a pulse width of 120 fs and a repetition rate of 1 kHz were divided into two beams, and one was used for pumping the sample with a time delay. The other part was used as a probe beam and the reflected light was detected by a photo diode in measurements of time response at 800 nm. Some measurements were done with second harmonic light from a

beta barium borate crystal inserted in either the pump or probe beam path. The laser spot sizes of the beams on the sample surface were about 200 μm.

The measurements in the microsecond region were done with the same pumping source at a repetition rate of 1 kHz. For the probe beam, we used a quasi-continuous wave from a picosecond mode-locked Ti–sapphire laser. Rectangular pulses with a width of 300 ns (actually a pulse train with intervals of 12.5 ns) and an appropriate time delay were generated by an acoustic-optic modulator and used as a probe light.

The time-resolved spectra were taken by using a white light continuum from a sapphire block inserted in the probe beam path. The fundamental light at 800 nm was removed by an IR cut filter inserted just after the sapphire block. The reflectance spectra were taken with a grating monochromator equipped with a photomultiplier or a photodiode, depending on the wavelength. The pumping light was modulated by a mechanical chopper at a frequency one half of the repetition rate of the amplified pulses, and the signals were registered by a lock-in amplifier.

The steady-state spectra of the reflectance were measured by using a conventional micro-spectrometry set-up (Jasco Corporation). In order to avoid modification of the optical alignment due to thermal expansion of the cryostat, the temperature of the sample was controlled by a small electric heater of several millimetres mounted on the cold finger without changing the temperature of the cryostat itself. This method allows us to change the temperature from 25 to 300 K in several minutes without any detectable shift of the sample position.

3. Results

The reflectance spectra in $E \parallel a$ and $E \parallel b$ polarizations are shown in figure 1. The step structure at 4 eV for the $E \parallel b$ configuration is caused by changing of the light source in the spectrometer. The gross features of the spectra are in agreement with the previous report [12], though the absolute values of the reflectance are about one half of the reported values because of the loss of the reflected light due to surface roughness. The most pronounced feature around 1 eV has been assigned as $d^{+}_{xy} \rightarrow d_{xz}$ and $d^{+}_{xy} \rightarrow d_{yz}$ [12] or charge transfer between two V ions on the rung [18] or on-rung doublet–doublet (originating from a 3d(V)–2p(O)–3d(V) resonance) transition [19]. The shoulder around 1.25 eV was assigned to the d–d transition of V^{4+} ions [12, 20]. The second pronounced feature, i.e., a broad peak around 3.2 eV in the $E \parallel a$ configuration, has been assigned as $d^{+}_{xy} \rightarrow d_{x^2-y^2}$ in the V d block excitation [12] or 2p(O)–3d(V) charge transfer transition [20]. The rather structureless continuum in visible region can be ascribed to various d–d transitions of vanadium ions. The main changes of the spectra on increasing the temperature are the decrease of the peak intensity near 1 eV in both polarizations, the emergence of a hump structure at 1.55 eV in the $E \parallel b$ polarization, and an increase of the intensity from 1.2 to 4 eV in the $E \parallel b$ polarization.

To reveal the precise temperature dependence of the reflectance at each photon energy, we performed temperature-scan measurements at some fixed wavelengths, shown by arrows in figure 1. The temperature was changed from 25 K, which is reasonably below T_c, to room temperature, and the reflectance values normalized by the value at 25 K were calculated and are shown in figure 2. The phase transition is most clearly seen at 1.7 eV in a-polarization. This curve is in good agreement up to 50 K with the temperature dependence of the band intensity integrated between 1.4 and 1.8 eV reported by Long *et al* [12]. The reflectance increases rapidly above 50 K and reaches 1.7 times the initial value at 300 K. The steep decreases in reflectance at T_c are found at 1.55 eV for both polarizations, while a slight increase was found for b-polarization at 3.0 eV. In all cases, gradual changes either decreasing or increasing are found between 50 K and room temperature.

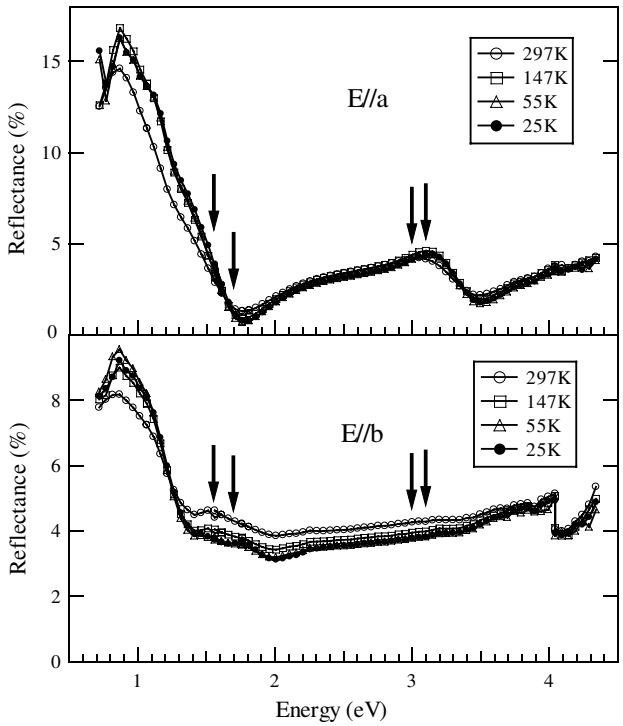

Figure 1. Reflectance spectra of an α'-NaV_2O_5 single crystal at 25 K (solid circles), 55 K (open triangles), 147 K open squares) and 297 K (open circles) in steady-state measurements. Upper and lower panels show the spectra in $E \parallel a$ and $E \parallel b$ polarizations, respectively. The arrows indicate the energies where the temperature dependence or transient response was measured. The step at 4 eV in the $E \parallel b$ spectra is an artefact due to changing of the light source from a tungsten lamp to a deuterium lamp.

The transient response of the reflectance at various polarizations, excitation intensities and detection wavelengths were measured at 4 K, and the relative changes of the reflectance ($\Delta R/R$) are presented in figures 3 and 4. The typical pulse energies for the pump and probe pulses were 1 and 0.2 μJ, which correspond to 2 and 0.4 mJ cm^{-2} per pulse, respectively. In these figures, the origin of the time axis is not calibrated. As the observed curves sometimes have background components before $t = 0$, probably due to a prepulse excitation by the amplified pulse with one cycle less round trip, the vertical positions are adjusted to the zero level line before $t = 0$.

Figure 3 shows the results for 1.55 eV pump and 1.55 eV probe in two polarization configurations *a*–*b* (*a* and *b* denote the polarization of the pump and probe beams, respectively) and *b*–*a* polarization.

As shown in figure 3(A), the response is negative at the lowest excitation (0.03 μJ) and the polarity switches to positive around 0.8 μJ in *a*–*b* polarization, while the response is always negative in *b*–*a* polarization. The change is as large as 7% at 4 μJ in *b*–*a* polarization. It should be noted that a slow modulation with a period of about 60 ps is superposed at 4 μJ excitation. The details of the rising waveforms in a shorter timescale are shown in (C) and (D). The negative build-up at 0.03 and 0.1 μJ shows a slow rising in about 3 ps. The pulse energy 0.1 μJ corresponds to 0.2 mJ cm^{-2}, which is 1000 times higher than the fluence in the measurements with the oscillator excitation (2 mW, 100 μm spot size, 80 MHz repetition) [15, 21]. In spite

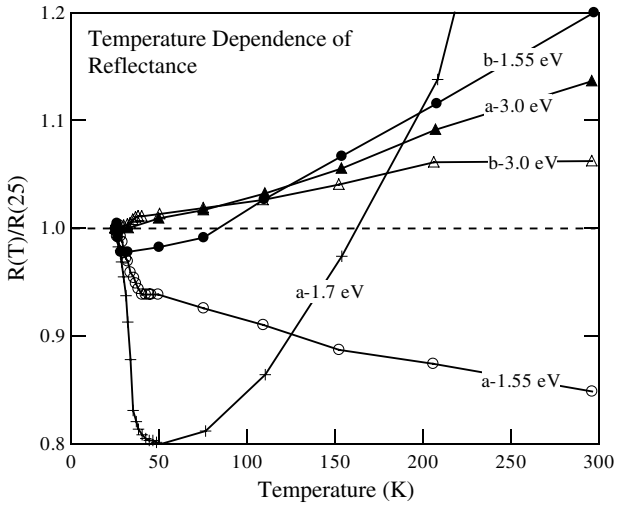

Figure 2. Temperature dependence of steady-state reflectance at 1.55, 1.7 and 3.0 eV normalized by the value at 25 K. The labels *a* and *b* denote the polarization.

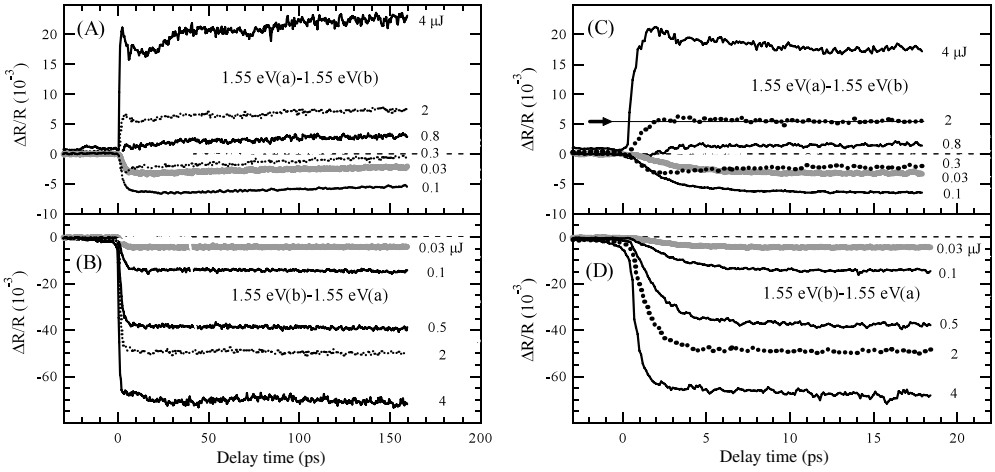

Figure 3. Time evolutions of the reflectance change at various excitation densities measured with 1.55 eV light for both pump and probe at 4 K for two polarization configurations: (A) *a*–*b* polarization and (B) *b*–*a* polarization. Their photon energies and respective polarizations (*a* or *b*) are indicated in the form 'pump (polarization)–probe (polarization)'. The numbers on the right of the curves indicate the excitation pulse energy in units of μJ. (C) and (D) show details of the rising part.

of three orders of magnitude difference in excitation density, the response is very similar to the case of oscillator excitation, and suggests the thermal origin of the reflectance change. In increasing the pumping power, another component with a faster rise time appears with opposite polarity in *a*–*b* polarization. In *b*–*a* polarization, the rise time is equally fast at 4 μJ.

Reflectance changes at 3.1 eV are shown in figure 4, where the response is always positive for *a*–*b* polarization, while it changes polarity at around 3 μJ for *b*–*a* polarization. Oscillating features appear with a higher contrast and a shorter period, about 30 ps ((A) and (B)). As

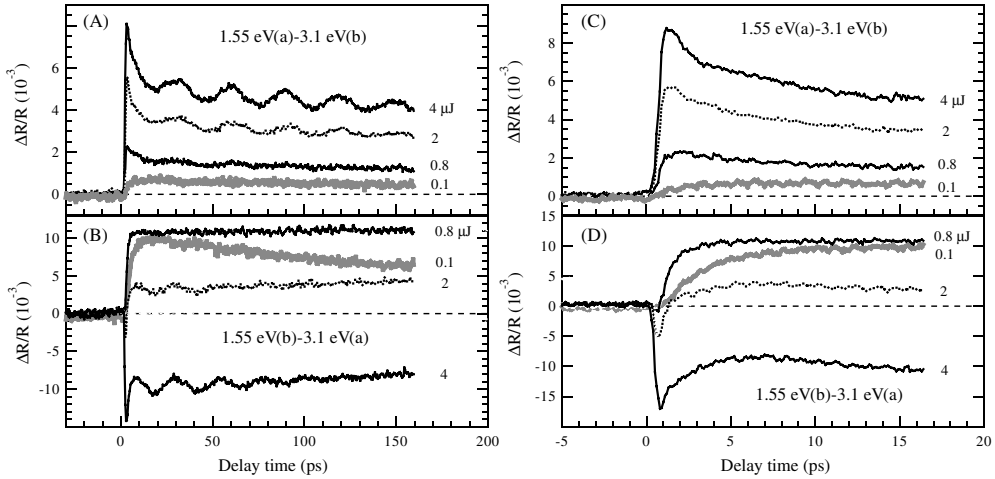

Figure 4. Time evolutions of the reflectance change at various excitation densities measured with 1.55 eV light for the pump and 3.1 eV light for the probe at 4 K for two polarization configurations: (A) *a–b* polarization and (B) *b–a* polarization. The numbers on the right of the curves indicate the excitation pulse energy in units of μJ. (C) and (D) show details of the rising part.

seen in (C) and (D), the rising time under weak excitation (0.1 μJ) is about 3 ps, which again suggests the thermal origin, while the response is very fast at a 4 μJ excitation.

The spectra of the transient reflectance change were measured at 4 K by using a white light continuum from a sapphire block with a pump intensity of 4 μJ. The reflectance change ΔR was evaluated from the average between the first peak and $t = 20$ ps for each time response curve. The relative changes of the reflectance ($\Delta R/R$) are shown in figures 5(A) and (B) for 1.55 and 3.1 eV excitations, respectively. A Si photodiode or a photomultiplier was used in the regions 1.4–2.3 eV (open circles) and 1.9–3.1 eV (solid circles), respectively. The curves shown in figure 5(C) are the difference spectra in steady-state measurements normalized by the reflectance at 25 K, i.e. $\{R(T) - R(25)\}/R(25)$, calculated from the data in figure 1. Corresponding data for *b–a* polarization are shown in figures 5(D)–(F).

4. Discussion

4.1. Interpretation of temporal behaviour

First, we discuss the effect of heating associated with the laser irradiation. In figure 5, we can notice a close resemblance between the transient spectra for 1.55 eV excitation and the steady-state temperature difference spectra. This suggests that the situation of the sample realized 10 or 20 ps after excitation is something like the high-temperature phase at room temperature as far as the electronic structure is concerned. To understand the overall behaviour of heating, we measured the reflectance change at 1.55 eV up to the microsecond region as shown in figure 6, where the responses before 150 ps are essentially the same as those shown in figures 3(A) and (B). The response is positive for *a–b* polarization and negative for *b–a* polarization. If the final temperature is close to room temperature, this is consistent with the temperature-scan curves in figure 2.

After 1 μs, the reflectance change becomes negative in *a–b* polarization and returns to the initial value after 10 μs, while it does not change sign in *b–a* polarization at all times. These behaviours are consistent with the temperature-scan curves in figure 2; that is, the reflectance

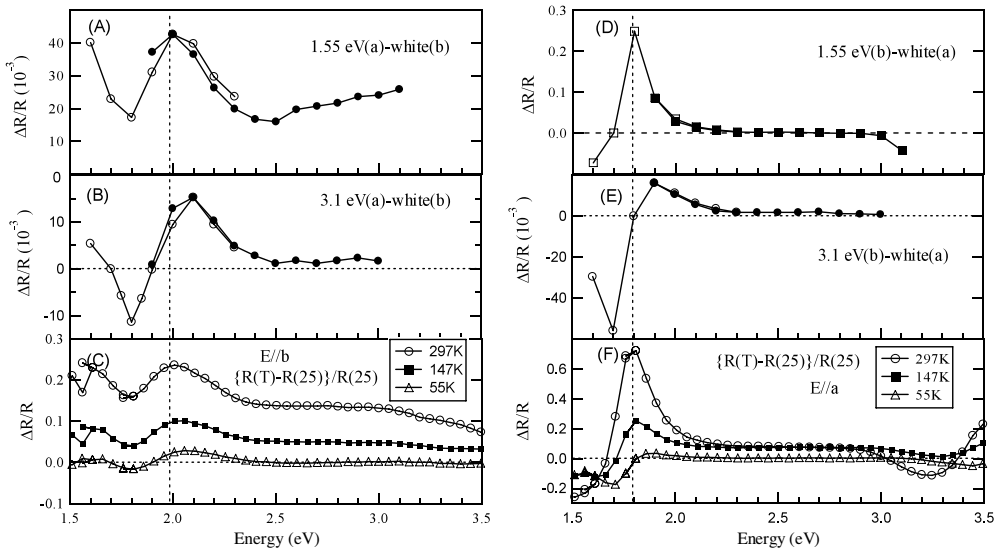

Figure 5. (A) and (B) are the spectra of the transient relative reflectance change ($\Delta R/R$) in *a*–*b* polarization under 4 μJ excitation at 1.55 and 3.1 eV, respectively, measured at 4 K. The values are evaluated within 20 ps from excitation (see the text for details). Panel (C) shows the difference spectra at 55, 147 and 297 K (deviation from the spectrum at 25 K normalized by the spectra at 25 K). The vertical broken lines show the peak position of the difference spectrum at 297 K. (D) and (E) are the spectra of the transient relative reflectance change ($\Delta R/R$) in *b*–*a* polarization under excitation at 1.55 eV and 3.1 eV, respectively. Panel (F) shows the difference spectra at 55, 147 and 297 K. The vertical broken lines show the peak position of the difference spectrum at 297 K.

change at 1.55 eV is always negative for *a*-polarization, while it is negative between 30 and 80 K for *b*-polarization. We can know that the temperature is 80 K at $t = 0.7$ μs from the zero crossing point in figure 6(A).

The heat energy is released from the excited electronic state and deposited in a thin layer at the surface within a penetration depth of the pumping light. The penetration depth for 800 nm light is 140 nm for both *a*- and *b*-polarizations and those for 400 nm light are 50 and 120 nm for *a*- and *b*-polarizations, respectively[1]. Then the heat will diffuse to the backside of the sample following the diffusion equation, and the temperature at the surface decreases. These slow changes in the microsecond scale are attributed to the cooling process due to the heat diffusion.

We can estimate the maximum temperature after photo-excitation by comparing the response curves in figure 3(A) with figure 2. The polarity of reflectance change after establishment of equilibrium (around 150 ps) goes from negative (0.03–0.3 μJ) to positive above 0.3 μJ, suggesting that the temperature at 150 ps is about 80 K for 0.3 μJ excitation. Figure 7 shows the heat capacity [22] and its integration between 0 and T K, which is the heat energy necessary for increasing the temperature from absolute zero to T K in units of R K, where, $R = 58.314$ J K^{-1} mol^{-1} is a gas constant. As seen from figure 7, the heat energy per unit volume at 80 K is about $198R$ K and that for 4 μJ is estimated to be 4/0.3 times this value, i.e., $2640R$ K, which means a final temperature of 270 K. This value seems reasonable, because the temperature increase is roughly estimated to be 350 K from the penetration depth 140 nm, excitation fluence 8 mJ cm^{-2} (at 4 μJ), and heat capacity 1.6 J cm^{-3} at room temperature. At this excitation intensity, the volume excitation density is about 3×10^{21} photons cm^{-3}.

[1] The penetration depth was calculated from the optical conductivity shown in [12].

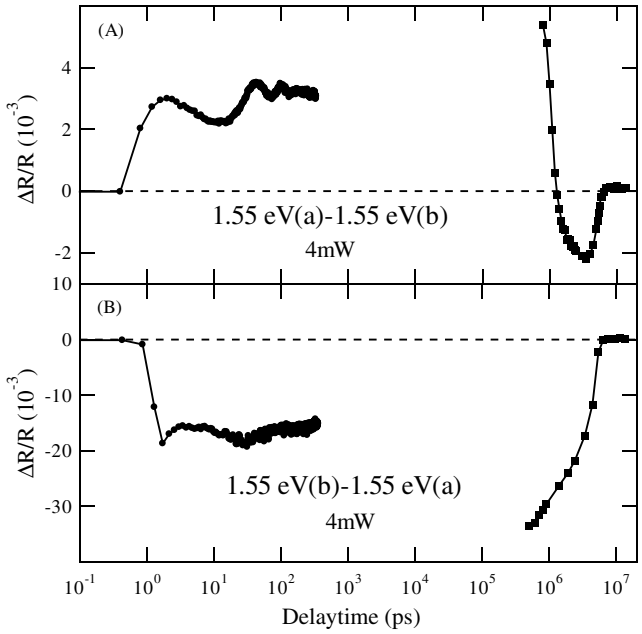

Figure 6. A logarithmic plot of long-time-range responses of the reflectance change with 1.55 eV light both for pump and probe. The response curves before 500 ps are taken in the same way as the curves in figures 3. The response curves in the microsecond region are taken with a quasi-continuous probe beam. Therefore, the absolute values in the ordinate in both time ranges may contain some inconsistency.

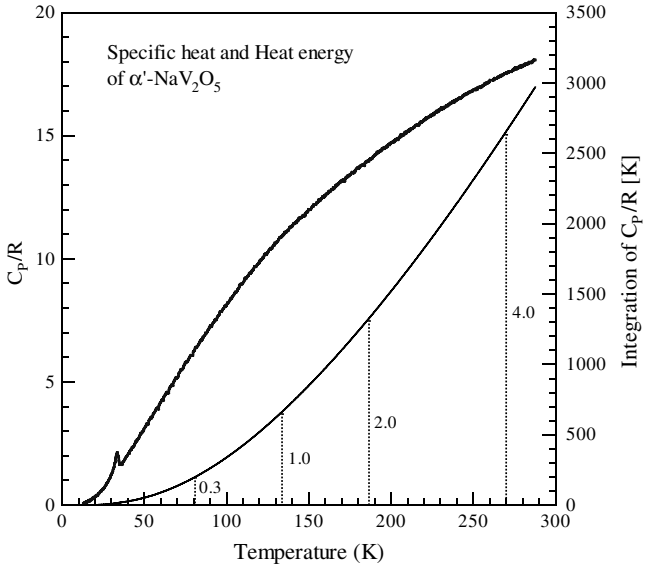

Figure 7. Temperature dependence of the specific heat reproduced from [12] (thick curve referenced to the left scale) and integrated specific heat (thin curve referenced to the right scale) of α'-NaV_2O_5. The ordinate scale on the left side is dimensionless as it is expressed as a ratio to the gas constant $R = 58.314\ \mathrm{J\,K^{-1}\,mol^{-1}}$. The vertical dotted lines are the estimated temperatures of the excited volume of the sample at respective excitation power indicated near the lines in units of μJ.

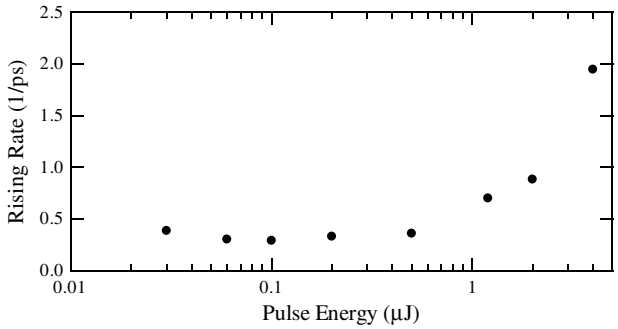

Figure 8. Rising rates of the transient reflectance change for various excitation pulse energies. The rates are deduced from the fitting with exponential functions to the curves in figure 3(C) and some similar curves.

The temperature difference spectrum in figure 5(C) consists of a peak around 2.0 eV, a dip at 1.8 and a plateau above 2.4 eV. The peak moves to lower energy on increasing the temperature. The signal at the dip is negative at low temperatures but is positive at temperatures higher than 147 K. Thus the spectrum in figure 5(A) is consistent with the estimated temperature, 270 K. From this evidence, we can conclude that the final temperature of the sample at the surface is approximately 270 K under 4 μJ, 1.55 eV excitation.

As already mentioned, for low-intensity excitation with mode-locked pulses, the response time, 3–5 ps, corresponds to the time necessary for heat to be released from the excited electronic states. However, at a higher excitation, 4 μJ, the final value of reflectance is settled within a very short time, as seen in figures 3(C), (D) and figures 4(C), (D). The rising (either to positive or negative directions) rates for the curves in figure 3(C) are deduced by fitting the curves with exponential functions, and are shown in figure 8. The rate is almost constant below 1 μJ, but it increases rapidly above this pulse energy and reaches 2 ps^{-1}, which corresponds to a time constant of 500 fs, at 4 μJ. As the time constant of heat releasing is 3 ps, it requires 3 (ln 2) $\approx$ 2 ps for one half of the heat energy to be released from the excited electronic states. Therefore, if $\Delta R/R$ were caused by heating, it would take 2 ps for the 4 μJ curve to arrive at the final value for the 2 μJ curve. However, as seen in figure 3(C), it takes only about 150 fs (limit of time-resolution) for $\Delta R/R$ to reach the final value of 2 μJ (horizontal arrow). This clearly shows that the response cannot be ascribed to the thermal effect. The fast rise is commonly seen above 2 μJ for all the response curves in figures 3 and 4.

From these facts we conclude that the very fast reflectance change at higher fluence is non-thermal. Incidentally, the complicated waveforms with a dip and a positive swing at 2 μJ in figure 4(D) and at 0.8 μJ in figure 3(C) are ascribed to a superposition of low- and high-fluence schemes due to spatial inhomogeneity of the pumping beam on the sample surface.

The transient reflectance change spectrum under 3.1 eV excitation has a different shape compared to that for 1.55 eV excitation, as shown in figure 5(B); that is, the peak position is shifted to higher energy and the dip at 1.8 eV has a negative value. This spectrum is similar to the steady-state spectrum at 55 K shown in figure 5(C). In (E), also, the spectrum under 3.1 eV excitation corresponds to 55 K (F) rather than the 147 K or 297 K spectra. This is probably ascribed to the lower excitation density due to lower beam quality of the second harmonics.

4.2. Coherent oscillation

At higher fluences, above 2 μJ, where the non-thermal effect appears, the reflectance shows oscillatory structures (see figure 3(A)). The oscillating component in *a–b* polarization with

1.55 eV pump and 1.55 eV probe taken with a higher S/N ratio (not shown) is well fitted with a damped sinusoidal wave with a period of 60 ± 1 ps. The oscillation period obtained from a fitting to the curve for 3.1 eV probe (figure 4(A)) is 29.5 ps. Thus the period is proportional to the wavelength of the probe light. Similar behaviour has been found in some PIPT materials [4, 5, 23] and attributed to interference of the reflected probe light from the surface and the wavefront of the acoustic phonon burst, which propagates into the sample at a speed of an acoustic phonon, v. The period of oscillation observed in the pump and probe measurements, τ, is given by

$$\tau = \frac{\lambda_0}{2nv},$$

where n is the refractive index, and λ_0 is the wavelength of the probe light in vacuum.

Using $n = 1.42$ at 800 nm [12], we obtain $v = 4.7$ km s^{-1}, which is a reasonable value for oxide crystals.

4.3. Ultrafast non-thermal effect

The observed phenomena are similar to laser annealing in semiconductors [1]. The melting process is understood in a sequence starting from carrier excitation followed by thermalization, carrier diffusion, thermal diffusion and resolidification. The physics of thermal melting is well understood and believed to occur in several picoseconds, and the temperature reverts back to the ambient value on the timescale of microseconds [1]. It has been proven in many materials by means of various time-resolved measurements. The dynamics of laser-induced melting was studied by means of time-resolved reflectance in Si and GaAs [24], or in InSb [25]. Recently, the time-resolved x-ray diffraction method was applied to InSb [26].

In addition to the de-excitation time of the excited electronic state, the thermal phase transition will suffer further delay. To establish a thermal distribution in the phonon system needs at least the phonon lifetime, which is roughly estimated from the Raman line widths of phonon modes. As the line width is 1 to 10 cm^{-1} in ordinary solids, the time constant will be several picoseconds. If these parameters do not depend on the excitation intensity, it is hard to understand a process which occurs within one picosecond as a thermal effect. Therefore, the phase transition or melting which occurs within several hundred femtoseconds is usually categorized as a non-thermal process. Similarly, in our case, the fast rising cannot be explained as a thermally induced phenomenon, but should be ascribed to a non-thermal process. As the transient spectra in figure 5 show, the photo-generated state is similar to that at room temperature, regardless of the creation mechanism being either thermal or non-thermal. The action of the pumping pulse is to cause d–d transitions within V ions and/or charge transfer excitations among V ions or between V and O ions. The charge transfer excitation will cause a disordered charge distribution on the vanadium sublattice. If the density of such a disordered area is sufficiently high, the whole vanadium system might be able to be converted into a state with a completely homogeneous charge distribution directly from the excited electronic states before heating of the lattice.

5. Summary

We investigated the transient reflectance change induced by photo-excitation in α'-NaV_2O_5. At relatively low excitation fluence, the response takes several picoseconds, and it becomes very fast at higher excitation fluence. The temporal response from the femtosecond to the microsecond region was carefully compared to the temperature dependence of the reflectance of this material, and we concluded that the slow response in the picosecond region is fully

ascribed to a transient increase of temperature within the excited volume of the sample, while the response within a picosecond should be assigned to a non-thermal effect. We observed no appreciable difference in the spectral shape of the photocreated states, irrespective of the production process. Our results suggest that the charge-disordered state is created directly from the excited electronic states without necessitating lattice heating.

Acknowledgments

The micro-reflectance measurements were done using the facility of the spectroscopy laboratory at ISSP. This work has been supported by a Grant-in-Aid for Scientific Research (A) and (B) from the Ministry of Education, Culture, Sports, Science and Technology of Japan.

References

[1] Sundaram S K and Mazur E 2002 *Nat. Mater.* **1** 217
[2] Koshihara S, Tokura Y, Mitani T, Saito G and Koda T 1990 *Phys. Rev.* B **42** 6853
[3] Iwai S, Tanaka S, Fujinuma K, Kishida H, Okamoto H and Tokura Y 2002 *Phys. Rev. Lett.* **88** 057402
[4] Tanimura K 2004 *Phys. Rev.* B **70** 144112
[5] Miyano K, Tanaka T, Tomioka Y and Tokura Y 1997 *Phys. Rev. Lett.* **78** 4257
Fiebig M, Miyano K, Tomioka Y and Tokura Y 2000 *Appl. Phys.* B **71** 211
[6] Iwai S, Ono M, Maeda A, Matsuzaki H, Kishida H, Okamoto H and Tokura Y 2003 *Phys. Rev. Lett.* **91** 057401
[7] Ogasawara T, Kimura T, Ishikawa T, Kuwata-Gonokami M and Tokura Y 2001 *Phys. Rev.* B **63** 113105
[8] Nasu K (ed) 1997 *Relaxations of Excited States and Photoinduced Structural Phase Transitions* (*Springer Series in Solid State Science*) vol 124 (Berlin: Springer)
[9] Isobe M and Ueda Y 1996 *J. Phys. Soc. Japan* **64** 1178
[10] Seo H and Fukuyama H 1998 *J. Phys. Soc. Japan* **67** 2602
[11] Fujii Y, Nakao H, Yoshihama T, Nishi M, Nakajima K, Kakurai K, Isobe M, Ueda Y and Sawa H 1997 *J. Phys. Soc. Japan* **66** 326
[12] Long V C, Zhu Z, Musfeldt J L, Wei X, Koo H-J, Whangbo M-H, Jegoudez J and Revcolevschi A 1999 *Phys. Rev.* B **60** 15721
[13] Fischer M, Lemmens P, Els G, Güntherodt G, Sherman E Ya, Morre E, Geibel C and Steglich F 1999 *Phys. Rev.* B **60** 7284
[14] Popova M N, Sushkov A B, Klimin S A, Chukalina E P, Malkin B Z, Isobe M and Ueda Y 2002 *Phys. Rev.* B **65** 144303
[15] Suemoto T, Aiba M, Nakajima M, Isobe M and Ueda Y 2004 *Solid State Commun.* **130** 4951
[16] Suemoto T, Nakajima M, Kazumi K, Nagase H, Aiba M, Isobe M and Ueda Y 2005 *J. Phys. Conf. Series* **21** 15
[17] Nakajima M, Kazumi K, Isobe M, Ueda Y and Suemoto T 2005 *J. Phys. Conf. Series* **21** 201
[18] Damascelli A, van der Marel D, Grueninger M, Presura C, Palstra T T M, Jegoudez J and Revcolevschi A 1998 *Phys. Rev. Lett.* **81** 918
[19] Suaud N and Lepetit B 2002 *Phys. Rev. Lett.* **88** 056405
[20] Golubchik S, Isobe M, Ivlev A N, Mavrin B N, Popova M N, Sushkov A B, Ueda Y and Vasil'ev A N 1997 *J. Phys. Soc. Japan* **66** 4042
[21] Aiba M, Nakajima M, Isobe M, Ueda Y and Suemoto T 2005 *J. Lumin.* **112** 246
[22] Powell D K, Brill J W, Zeng Z and Greenblatt M 1998 *Phys. Rev.* B **58** R2937
[23] Tanimura K and Akimoto I 2001 *J. Lumin.* **94–95** 483
[24] Sokolowski-Tinten K, Bialkowski J and von der Linde D 1995 *Phys. Rev.* B **51** 14186
[25] Shumay I L and Hoefer U 1996 *Phys. Rev.* B **53** 15878
[26] Rousse A *et al* 2001 *Nature* **410** 65